Distinguishing Signatures of Multipathway Conformational Transitions

Christopher A. Pierse and Olga K. Dudko

Distinguishing Signatures of Multi-pathway Conformational Transitions

Christopher A. Pierse and Olga K. Dudko

Department of Physics, University of California at San Diego, La Jolla, California 92093, USA

(Dated: January 19, 2017)

The folding and binding of biomolecules into functional conformations are thought to be commonly mediated by multiple pathways rather than a unique route. Yet even in experiments where one can "see" individual conformational transitions, their stochastic nature generally precludes one from determining whether the transitions occurred through one or multiple pathways. We establish model-free, observable signatures in the response of macromolecules to force that unambiguously identify multiple pathways – even when the pathways themselves cannot be resolved. The unified analytical description reveals that, through multiple pathways, the response of molecules to external forces can be shaped in diverse ways, resulting in a rich design space for tailored biological function already at the single molecule level.

A hallmark of biological systems is their ability to tailor their function to a new environment [1]. Biological function is realized – and tuned in response to perturbation – through the conformational transitions of the constituent biomolecules [2]. The transitions occur through reaction pathways, each pathway defined as an ensemble of trajectories in configurational space that connect the initial and final conformations [3]. Considering that the energy of even a small protein is described by a rugged hypersurface – the energy landscape – in the space of several thousand coordinates, one should expect biomolecular folding and binding to be commonly mediated by more than one such pathway (Fig. 1) [4, 5].

Conformational transitions under the influence of external forces can be probed in real time in single-molecule experiments [6–9]. However, even when one has access to the conformational trajectories of a single molecule, stochasticity often precludes a one-to-one mapping of the individual trajectories to specific pathways. As a result, it generally remains unclear from the trajectories themselves whether the transitions occurred through one or multiple pathways. Given this ambiguity, how can one tell if conformational transitions are governed by multiple pathways? And to what extent can pathway multiplicity provide the design freedom for tailoring biomolecular function to a changed environment?

Through a unified analytical framework, we show that multiple pathways can be identified through a set of universal signatures in the response of the molecule to force – even when the pathways themselves cannot be resolved experimentally. The established signatures manifest themselves in experimentally accessible ranges of parameters. A spectrum of novel behaviors – multiple binding modes, enhanced or inhibited transition rate, extended working range, or robustness – is shown to emerge even in a minimal multi-pathway system.

Expressions for the measurable quantities. The force response of macromolecules is typically measured by stretching individual molecules with either a constant or ramping force [7]. Constant-force experiments report the force-dependent rate of transitions from the native folded/bound state(s) N to the unfolded/unbound state U. From the flux-over-population formulation of the reaction rate [10], we find that the net transition rate at any force F can be universally written as the weighted sum of the rates $k_i(F)$ along each pathway [11]:

$$k(F) = \sum_i w_i(F)k_i(F). \tag{1}$$

The weight $w_i(\{k_j(F)\}) \in [0,1]$ is the population-averaged fraction of the lifetime – or, equivalently, the steady-state fraction of the population [11, 12] – with access to pathway i.

Equation (1) is intuitive when pathways originate from a common N-state (Fig. 2a-f) as they supply transitions through their combined flux. Perhaps less intuitively, Eq. (1) holds even when pathways originate from disconnected N-states (Fig. 2g): the slowest pathway has the largest weight $w_i(F)$ ($\sim$ time), limiting the net transition rate.

Microscopically, transition rates are governed by activation barriers, which themselves change under force. The force-dependence of the rate $k_j(F)$ has been established analytically from Kramers theory for a single-barrier pathway in terms of its zero-force rate k_j^0 and
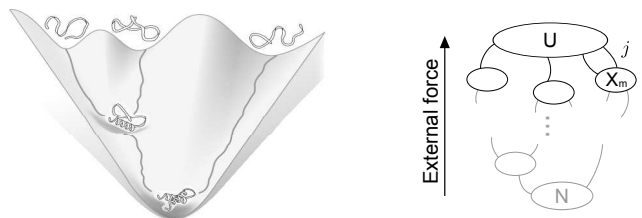

FIG. 1. A fragment of the energy landscape of a biomolecule with multiple reaction pathways connecting distinct conformational states. This Letter addresses the challenge of identifying the presence of multiple pathways and explores the functional advantages of pathway multiplicity.

barrier $\Delta G_j^\ddagger$ displaced from N by $x_j^\ddagger$ [13]:

$$k_j(F) = k_j^0 \left(1 - \frac{\nu_j F x_j^\ddagger}{\Delta G_j^\ddagger}\right)^{\frac{1}{\nu_j}-1} e^{\beta \Delta G_j^\ddagger \left[1-\left(1-\frac{\nu_j F x_j^\ddagger}{\Delta G_j^\ddagger}\right)^{\frac{1}{\nu_j}}\right]},$$

(2)

where $\beta \equiv 1/k_B T$ and ν_j parameterizes the shape of the barrier. For a multi-barrier pathway i, the net rate is determined by the rates $\{k_j(F)\}$ of the constituent single-barrier pathway segments. Together, Eqs. (1, 2) describe the evolution of the net transition rate with force when multiple pathways are present.

Force-ramp experiments report the distributions of transition forces, $p(F|\dot{F})$, at different force-loading rates $\dot{F}(F)$. To establish an analytical form of these distributions, we express $p(F|\dot{F})$ as the sum of the fluxes into U from all pathways:

$$p(F|\dot{F}) = \sum_i p_{path\,i}(F) = \sum_{m,j} \frac{k_{X_m \overset{j}{\to} U}(F)}{\dot{F}(F)} \phi_{X_m}(F).$$

(3)

Here, the second equality specifies the ingredients of each flux: the population $\phi_{X_m}(F)$ in a state X_m that is a single pathway segment j from U (Fig. 1), the transition rate $k_{X_m \overset{j}{\to} U}(F)$ of this segment, and the loading rate. The population $\phi_{X_m}(F) \in [0,1]$ is equivalent to the joint probability of having entered and not yet left X_m by the time force F is reached. As such, $\phi_{X_m}(F)$ is determined by the rates $\{k_j(F)\}$ and survival probabilities $\{S_j(F)\}$ of all segments that transmit population toward or away from X_m. $S_j(F)$ is the solution to the rate equation describing escape through segment j: $\frac{dS_j(F)}{dt} = -k_j(F)S_j(F)$. With $k_j(F)$ in Eq.(2) and the loading rate expressed through the stiffness and speed of the pulling device, $\dot{F} \approx \kappa_S V$, this equation is exactly solvable:

$$S_j(F) = \exp\left[\frac{k_j^0 - k_j(F)\left(1 - \nu_j F x_j^\ddagger/\Delta G_j^\ddagger\right)^{1-\frac{1}{\nu_j}}}{\beta \kappa_S V x_j^\ddagger}\right].$$

(4)

Having analytically established the key quantities, Eqs. (1-4), we can address the experimental identification and functional advantages of multiple pathways through a hierarchy of fundamental multi-pathway configurations.

a. Maximizing the transition rate by switching pathways. The simplest multi-pathway configuration consists of two pathways, each directly connecting N to U (Fig. 2a-b). The net rate, measurable in a constant-force experiment, is obtained from Eqs. (1, 2) with $w_i(F) = 1$: $k(F) = k_1(F) + k_2(F)$. The force distribution, measurable in a force-ramp experiment, is obtained from Eq. (3) with $X_m = N$, $k_{N \overset{1}{\to} U}(F) = k_1(F)$, $k_{N \overset{2}{\to} U}(F) = k_2(F)$, and $\phi_N(F) = S_1(F)S_2(F)$ being the probability of taking

neither pathway by force F. The contribution of pathway i to the force distribution in Eq. (3) is thus

$$p_{path\,i}(F) = \frac{k_i(F)}{\kappa_S V} S_1(F) S_2(F)$$

(5)

with $S_i(F)$ in Eq. (4).

Through the effect that force has on individual barriers, force can turn an intrinsically slow pathway into the dominant pathway. This switch in pathway dominance occurs if the high intrinsic barrier of the initially slow pathway is softer, $x_2^\ddagger > x_1^\ddagger$, and thus more compliant under force. The force at which the system switches pathways is found by asking, via Eqs. (1, 2), when the rates along the pathways become equal [11]:

$$F_{switch} \approx \frac{\ln\left(\frac{k_1^0}{k_2^0}\right)}{\beta(x_2^\ddagger - x_1^\ddagger)}\left[1 + \ln\left(\frac{k_1^0}{k_2^0}\right)\frac{\frac{(1-\nu_2)x_2^{\ddagger 2}}{\Delta G_2^\ddagger} - \frac{(1-\nu_1)x_1^{\ddagger 2}}{\Delta G_1^\ddagger}}{\beta(x_2^\ddagger - x_1^\ddagger)}\right].$$

(6)

Equations (1, 2) further predict that the pathway switch manifests itself as an anomalous upturn in the transition rate at F_{switch} (Fig. 2a) – a result of the crossover to the strongly force-dependent rate of the soft barrier.

In force-ramp experiments, the pathway switch yields a transient increase in the height of the force distribution with increasing loading rate (Fig. 2a), which contrasts the monotonic decrease characteristic of single-pathway transitions [11, 13]. The height increase originates from the softer barrier faced upon the switch: force lowers a softer barrier faster such that transitions are completed within a narrower force range. The evolution of the distributions with loading rate, including the anomalous height trend, is captured by the analytical theory, Eqs. (3, 5) (Fig. 2a). At low and high loading rates, where only one pathway dominates, the known single-pathway behavior is recovered [11, 13]. Other measurable signatures of a pathway switch include a sigmoidal variance and a downturn in the average force versus loading rate [11].

A functional advantage of switching pathways is the resulting transition rate, which is maximized over a significantly broader force range than what is possible with either pathway alone (Fig. 2a). Evidence of this scenario, an upturn in the rate, has been observed in SH3 [16], whose ability to switch conformations rapidly under cellular stresses is consistent with its role as a regulatory component of many signaling proteins.

b. Conforming to high force yet increasingly resisting low force. The pathway switch yields an intriguing behavior (Fig. 2b) when one pathway resists force, a consequence of its transition state being more compact than N: $x_i^\ddagger < 0$. Equations (1, 2) predict that, when a force-resistant pathway is dominant at zero force, but a force-compliant pathway takes over beyond F_{switch}, the switch produces a dip in the rate (Fig. 2b). This signature, observable in constant-force experiments, is the result of a
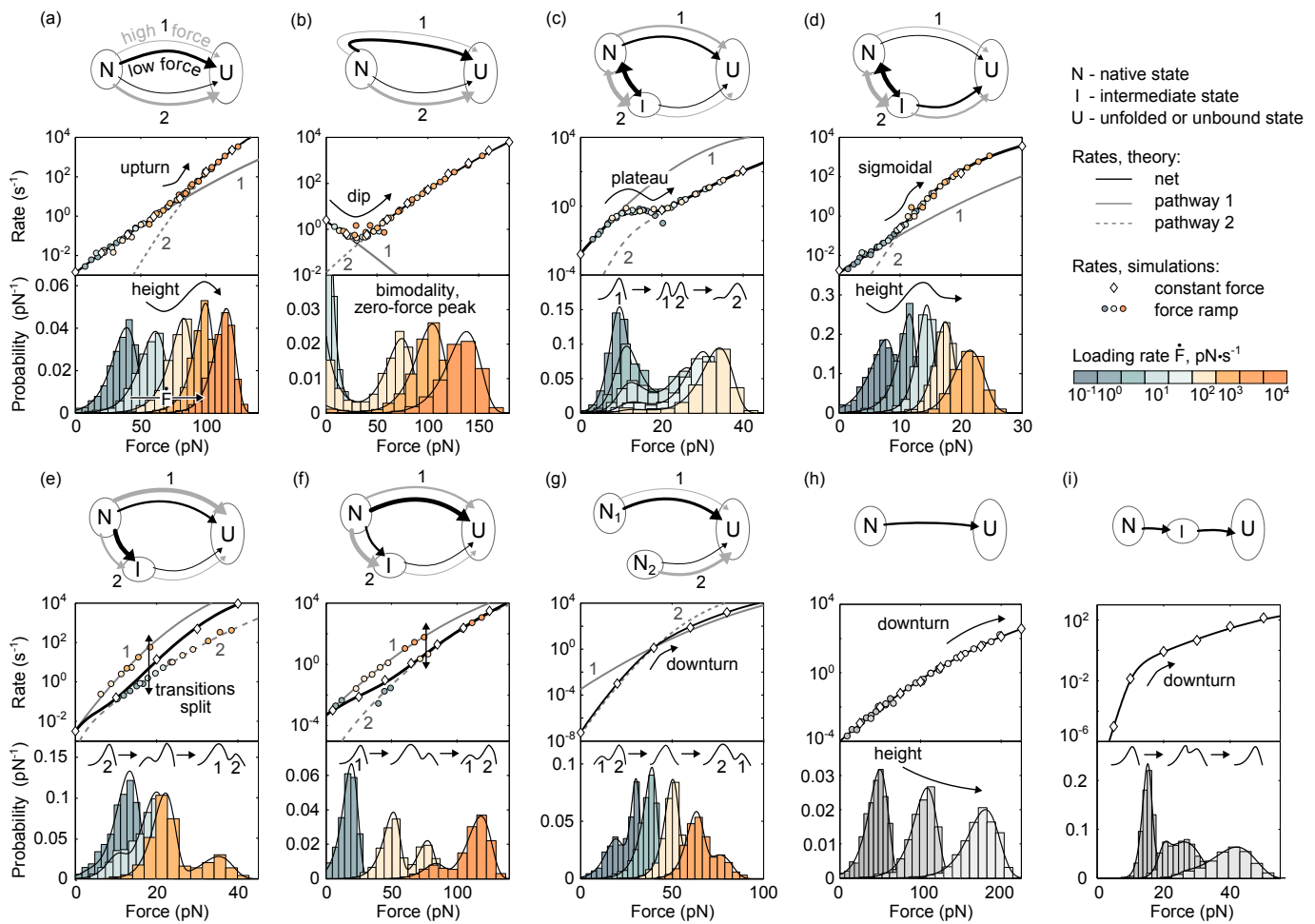
FIG. 2. Fundamental multi-pathway configurations: distinguishing signatures and functional advantages. Lines: theory. Histograms: simulations. Symbols: simulations, transformed histograms [14, 15]. (a) A pathway switch yields an upturn in the rate and a nonmonotonic trend in the force distributions with loading rate. The transition rate becomes maximized over a broad force range. (b) Switching from a force-resistant to a force-compliant pathway yields a dip in the rate and bimodal force distributions with a zero-force peak. The system rapidly dissociates under strong forces yet increasing resists weak forces. (c) An intermediate leading to a slow transition step under rapid $N - I$ exchange yields a plateau in the rate and bimodal force distributions. Transient insensitivity to perturbation is acquired. (d) An intermediate leading to a fast step yields a sigmoidal rate curve and a nonmonotonic trend in force distributions. Distinct binding modes are acquired. (e,f) An intermediate irreversibly sequestering population yields bimodal force distributions where the peaks dominate at different loading rates. The transitions become spread over broader time- and force-ranges. (g) Multiple native states yield a transient unimodality in the force distribution. The rate of transitions leaving the functional state becomes inhibited. (h,i) For reference: single-pathway transitions with one [13] and multiple [17] barriers with corresponding signatures.

crossover from the decreasing rate of the force-resistant pathway to the increasing rate of the force-compliant pathway.

In force-ramp experiments, the pathway switch is marked by distinct bimodality in the force distributions: the first peak remains at zero force under all loading rates (Fig. 2b). This peak originates from the force-resistant pathway, whose transition probability is highest when no force is applied.

The upturn and dip in the rate (Fig. 2a-b) are straightforward to distinguish from the opposite curvature characteristic of single-pathway transitions, either through

one [13] or multiple [17] barriers (Fig. 2h-i), even with rebinding. The sharpness of the upturn/dip distinguishes it from the gradual upturn accompanying the alignment of a pathway with the pulling direction [11, 18].

A combination of force-resistant and force-compliant pathways introduces a global minimum in the off-rate (Fig. 2b). This signature has been observed in experiments on leukocytes [19], where it creates a range of forces (shear stresses) at which leukocytes can adhere to blood vessel walls for long enough to roll and search for inflammation.

c. Acquiring robustness through a plateau in the rate. Moving up in complexity, consider an intermediate state I on one pathway (Fig. 2c-f). The net transition rate from Eq. (1) is $k(F) = \{1 + k_{NI}(F)/[k_{IU}(F) + k_{IN}(F)]\}^{-1} k_1(F) + k_2(F)$ with the rate of the intermediate-containing pathway $k_2(F) = [1 - w_1(F)] k_{IU}(F)$ and weights $w_{1,2}(F)$ specified in Table S1 [11]. Here, $w_2(F) = 1$, but $w_1(F) < 1$ as pathway 1 is only accessible from N. When the intermediate is short-lived, $k_{IU}(F) \gg k_{NI}(F)$, the net rate of configurations a-b is recovered. Otherwise, new behaviors emerge (Fig. 2c-f), dictated by the relative speeds of $N - I$ exchange and transitions into U.

Under fast $N - I$ exchange $(k_{NI}(F), k_{IN}(F) \gg k_1(F), k_{IU}(F))$, N and I remain in equilibrium at all forces (Fig. 2c-d). When I is separated from U by a high barrier, $k_{IU}(F) \ll k_1(F)$, I becomes a transient trap. Equations (1, 2) reveal that this trapping produces a plateau in the net transition rate (Fig. 2c). The plateau sets in at the force where transitions into U from the fast pathway subside, $w_1(F_{plateau}) \approx 1/2$, because the population instead accumulates in I [11]:

$$F_{plateau} \approx \frac{\ln\left(k_{IN}^0/k_{NI}^0\right)}{\beta(x_{NI}^\ddagger - x_{IN}^\ddagger)}. \qquad (7)$$

The force distribution is obtained from Eq. (3) (Table S1) with $\{X_m\} = \{N, I\}$ and the populations $\phi_{X_m}(F)$ each being the probability of residing in state X_m and having not yet transitioned into U. Treating $N - I$ as one effective state with two pathways of rates $w_1(F)k_1(F)$ and $w_2(F)k_2(F)$, we can write the contributions from each pathway analogously to Eq. (5):

$$p_{path\,i}^{eq}(F) = \frac{w_i(F)k_i(F)}{\kappa_S V} S_1^{eq}(F) S_2^{eq}(F), \qquad (8)$$

where $S_i^{eq}(F)$ is found by solving $dS_i^{eq}(F)/dF = -w_i(F)k_i(F)S_i^{eq}(F)$ [11]. Equations (3, 8) reveal that the transient trapping causes bimodality in the force distributions that emerges at intermediate loading rates (Fig. 2c), $\dot{F} \approx \sqrt{2}k_1(F_{plateau})/\left[\beta(x_{NI}^\ddagger - x_{IN}^\ddagger)\right]$ [11]. The low-force peak, the sole peak at low loading rates, reflects transitions via the fast pathway. The high-force peak reflects transitions via the alternative pathway with I as the new source.

A plateau in the rate (Fig. 2c) provides robustness, or transient insensitivity to perturbation, at the single molecule level.

d. Acquiring distinct binding modes through a sigmoidal rate curve. Alternatively, when I is separated from U by a small barrier, $k_{IU}(F) \gg k_1(F)$, I provides access to a faster transition step (Fig. 2d). At low forces, the population predominantly transitions via $N \to U$. At intermediate forces, the population spends increasingly more time in I with access to the fast step $I \to U$,

resulting in a steep growth in the rate. At high forces, I becomes sufficiently stable to accumulate the remaining population, ending this steep growth. These three regimes produce a sigmoidal rate curve measurable in constant-force experiments (Fig. 2d).

In force-ramp experiments, an I that provides access to a fast transition step yields a nonmonotonic trend in the force distributions with loading rate (Fig. 2d). This anomaly, captured by Eqs. (3, 8), can be distinguished from configuration a [11].

A sigmoidal rate curve introduces two operating modes, a binding mode at low forces (low off-rate) and a dissociation mode at high forces (high off-rate). This effect is analogous to cooperative binding, as in the classic sigmoidal oxygen-hemoglobin binding curve [1], yet is achieved here without the need for cooperative ligands.

e-f. Broadening the range of resistance to stress by delaying transitions. When $N - I$ transitions are instead rare, $N \to I$ is essentially irreversible on the experimental timescale. When $k_{IU}(F) \gg k_{NU}(F)$, we recover configuration a (Fig. 2a). However, when $k_{IU}(F) \ll k_{NU}(F)$, I irreversibly sequesters a portion of the population, delaying its arrival into U (Fig. 2e-f). Unlike equilibrium trapping (Fig. 2c), both pathways are utilized even when one is significantly faster.

Under constant force, this sequestration substantially reduces the net transition rate even if only a few transitions seep into I. When $k_{NI}(F) > k_{NU}(F)$, the net rate drops close to the rate of the slow, intermediate-containing pathway, $k_2(F)$ (Fig. 2f). However, even when $k_{NI}(F) \ll k_{NU}(F)$, i.e. the sequestering effect is weak, the net rate does not reach the rate of the fast pathway, $k_1(F)$ (Fig. 2e). The irreversible splitting of the population between N and I yields a distinct, double-exponential decay in the survival probability $S_{N+I}(t)$ [11].

Under a force-ramp, the force distribution is obtained from Eq. (3) (Table S1) with the population in N, $\phi_N(F)$, being the probability of neither taking pathway 1 nor entering pathway 2 by force F. The population in I, $\phi_I(F)$, is the product of the probabilities of transitioning into I, $k_{NI}(F')S_{NI}(F')S_1(F')/\dot{F}(F')$, and remaining there until force F, $S_{IU}(F)/S_{IU}(F')$; integration over F' includes all transitions into I at forces $F' \leq F$. The resulting pathway contributions,

$$p_{path\,1}^{ir}(F) = \frac{k_1(F)}{\kappa_S V} S_1(F) S_{NI}(F), \qquad p_{path\,2}^{ir}(F) =$$
$$\frac{k_{IU}(F)}{\kappa_S V} \int_0^F \frac{k_{NI}(F')S_{NI}(F')S_1(F')}{\kappa_S V} \frac{S_{IU}(F)}{S_{IU}(F')} dF', \qquad (9)$$

together produce a bimodal distribution (Fig. 2e-f), reflecting the irreversible splitting of the $N - I$ population. The evolution of the two peaks with the loading rate identifies the underlying kinetic scheme. Specifically, if $k_{NI}(F) > k_{NU}(F)$ at low forces and $k_{NU}(F) > k_{NI}(F)$

at high forces (sequestering at low forces), increasing the loading rate gives I less time to sequester population; consequently, the high-force peak shrinks while the low-force peak grows (Fig. 2e). Reversed rate inequalities (sequestering at high forces) result in the opposite trend (Fig. 2f).

By sequestering, and thus delaying, a fraction of transitions, the system resists stress over broader ranges of timescales and forces (Fig. 2e-f). Experiments on the blood-clotting protein von Willebrand factor reported the splitting of transitions and emerging bimodality in the force distributions [20], suggesting that the extended working range exhibited by this protein is realized through this multi-pathway mechanism.

g. Inhibiting the dissociation rate through multiple native-like states. N and I act as coexisting native states, N_1 and N_2, when both states are initially populated but $N-I$ transitions are negligible, $k_{NI,IN}(F) \approx 0$ (Fig. 2g). Equation (1) for the net transition rate measurable at constant force becomes (Table S1) $k(F) = [p_1/k_1(F) + p_2/k_2(F)]^{-1}$. The fraction p_i of population originating from N_i is readily obtained either as the fraction of transitions into U from N_i if the native states are experimentally distinguishable, or from a fit of the survival probabilities, $S(t) = \sum_i p_i e^{-k_i(F)t}$ [11]. While the net rate is limited by the slowest pathway, an originally fast pathway can become rate-limiting under force, producing a downturn in the net rate at F_{switch}, Eq. (6) (Fig. 2g).

In the force-ramp regime, the contributions from the individual pathways to the measurable force distribution are found from Eq. (3) (Table S1):

$$p_{path\,i}^{mult\,N}(F) = p_i \frac{k_i(F)}{\kappa_S V} S_i(F). \tag{10}$$

Each contribution is an independent, unimodal single-pathway distribution. Their superposition exhibits bimodality, interrupted by transient unimodality at intermediate loading rates (Fig. 2g), which distinguishes these distributions from those of a single-barrier pathway (always unimodal [13], Fig. 2h) or a multi-barrier pathway (bimodal only at intermediate loading rates [17], Fig. 2i).

Multiple native states diversify the response to perturbation while inhibiting the rate of leaving the functional state (Fig. 2g). A ribozyme, an RNA that catalyzes reactions, was found to possess multiple native states [21, 22], which may underlie its ability to operate on multiple timescales.

The diverse spectrum of force-responses revealed through these minimal multi-pathway configurations provides a foundation for understanding more complex systems. Indeed, each additional pathway will produce an additional signature from the repertoire in Fig. 2 if the transition rates dominate over different ranges of force [11]. Considering that force enters the theory as a generic bias field imposed on the conformational dynamics, these findings should remain relevant under other types of perturbations, such as a chemical denaturant [23] or electric field [24].

[1] W. Bialek, Biophysics: Searching for Principles, (Princeton University Press, 2012).

[2] B. Alberts et al., Molecular Biology of the Cell, (Garland Science, New York, 2008).

[3] P.G. Bolhuis, D. Chandler, C. Dellago, and P.L. Geissler, Transition path sampling: throwing ropes over rough mountain passes, in the dark, Annu. Rev. Phys. Chem. **53**, 291 (2002).

[4] J.N. Onuchic, Z. Luthey-Schulten, and P.G. Wolynes, Theory of protein folding: the energy landscape perspective, Annu. Rev. Phys. Chem. **48**, 545 (1997).

[5] K.A. Dill and H.S. Chan, From Levinthal to pathways to funnels, Nat. Struct. Biol. **4**, 10 (1997).

[6] H. Kim and T. Ha, Single-molecule nanometry for biological physics, Rep. Prog. Phys. **76**, 016601 (2013).

[7] E. Evans, Probing the relation between force - lifetime - and chemistry in single molecular bonds, Annu. Rev. Biophys. Biomol. Struct. **30**, 105 (2001).

[8] K.C. Neuman and A. Nagy, Single-molecule force spectroscopy: optical tweezers, magnetic tweezers and atomic force microscopy, Nature Methods **5**, 491 (2008).

[9] M.T. Woodside and S.M. Block, Reconstructing folding energy landscapes by single-molecule force spectroscopy, Annu. Rev. Biophys. **43**, 19 (2014).

[10] P. Hänggi, P. Talkner, and M. Borkovec, Reaction-rate theory: fifty years after Kramers, Rev. Mod. Phys. **62**, 251 (1990).

[11] See Supplemental Material at [url] for details on the derivations of analytical results, simulations, and practical implementation of the established distinguishing signatures.

[12] P. Reimann, G. J. Schmid, and P. Hänggi, Universal equivalence of mean first-passage time and Kramers rate, Phys. Rev. E. **60**, R1 (1999).

[13] O.K. Dudko, G. Hummer, and A. Szabo, Intrinsic rates and activation free energies from single-molecule pulling experiments, Phys. Rev. Lett. **96**, 108101 (2006).

[14] O.K. Dudko, G. Hummer, A. Szabo, Theory, analysis, and interpretation of single-molecule force spectroscopy experiments, Proc. Natl. Acad. Sci. USA **105**, 15755 (2008).

[15] Y. Zhang and O. K. Dudko, A transformation for the mechanical fingerprints of complex biomolecular interactions, Proc. Natl. Acad. Sci. U.S.A. **110**, 16432 (2013).

[16] E. J. Guinn, B. Jagannathan, and S. Marqusee, Single-molecule chemo-mechanical unfolding reveals multiple transition state barriers in a small single-domain protein, Nat. Commun. **6**, 6861 (2012).

[17] A. Garai, Y. Zhang, and O. K. Dudko, Conformational dynamics through an intermediate, J. Chem. Phys. **140**, 135101 (2014).

[18] Y. Suzuki and O. K. Dudko, Single-molecule rupture dynamics on multidimensional landscapes, Phys. Rev. Lett. **104**, 048101 (2010).

[19] B.T. Marshall, M. Long, J.W. Piper, T. Yago, R.P. McEver, and C. Zhu, Direct observation of catch bonds involving cell-adhesion molecules, Nature **423**, 190 (2003).

[20] J. Kim, C.Z. Zhang, X. Zhang, and T. A. Springer, A mechanically stabilized receptor-ligand flex-bond important in the vasculature, Nature **466**, 992 (2010).

[21] S. V. Solomatin, M. Greenfeld, S. Chu, and D. Herschlag, Multiple native states reveal persistent ruggedness of an RNA folding landscape, Nature **463**, 681 (2010).

[22] B. P. Paudel and D. Rueda, Molecular crowding accelerates ribozyme docking and catalysis, J. Am. Chem. Soc., **136**, 16700 (2014).

[23] A. R. Fersht, L. S. Itzhaki, J. Matthews, and D. Otzen, Single versus parallel pathways of protein folding and fractional formation of structure in the transition state, Proc. Natl. Acad. Sci. U.S.A. **91**, 10426 (1994).

[24] O.K. Dudko, J. Mathe, A. Szabo, A. Meller, and G. Hummer, Extracting Kinetics from Single-Molecule Force Spectroscopy: Nanopore Unzipping of DNA Hairpins, Biophys. J. **92**, 4188 (2007).